

PDF hosted at the Radboud Repository of the Radboud University Nijmegen

The following full text is a publisher's version.

For additional information about this publication click this link.

<http://hdl.handle.net/2066/34957>

Please be advised that this information was generated on 2019-06-27 and may be subject to change.

Coupling of *Methanothermobacter thermautotrophicus* Methane Formation and Growth in Fed-Batch and Continuous Cultures under Different H₂ Gassing Regimens

Linda M. I. de Poorter, Wim J. Geerts and Jan T. Keltjens
Appl. Environ. Microbiol. 2007, 73(3):740. DOI:
10.1128/AEM.01885-06.
Published Ahead of Print 1 December 2006.

Updated information and services can be found at:
<http://aem.asm.org/content/73/3/740>

SUPPLEMENTAL MATERIAL

These include:

[Supplemental material](#)

REFERENCES

This article cites 36 articles, 14 of which can be accessed free
at: <http://aem.asm.org/content/73/3/740#ref-list-1>

CONTENT ALERTS

Receive: RSS Feeds, eTOCs, free email alerts (when new
articles cite this article), [more»](#)

Information about commercial reprint orders: <http://journals.asm.org/site/misc/reprints.xhtml>
To subscribe to to another ASM Journal go to: <http://journals.asm.org/site/subscriptions/>

Coupling of *Methanothermobacter thermautotrophicus* Methane Formation and Growth in Fed-Batch and Continuous Cultures under Different H₂ Gassing Regimens^{∇†}

Linda M. I. de Poorter, Wim J. Geerts, and Jan T. Keltjens*

Department of Microbiology, Faculty of Science, Radboud University of Nijmegen, Nijmegen, The Netherlands

Received 8 August 2006/Accepted 16 November 2006

In nature, H₂- and CO₂-utilizing methanogenic archaea have to couple the processes of methanogenesis and autotrophic growth under highly variable conditions with respect to the supply and concentration of their energy source, hydrogen. To study the hydrogen-dependent coupling between methanogenesis and growth, *Methanothermobacter thermautotrophicus* was cultured in a fed-batch fermentor and in a chemostat under different 80% H₂–20% CO₂ gassing regimens while we continuously monitored the dissolved hydrogen partial pressures (p_{H_2}). In the fed-batch system, in which the conditions continuously changed the uptake rates by the growing biomass, the organism displayed a complex and yet defined growth behavior, comprising the consecutive lag, exponential, and linear growth phases. It was found that the in situ hydrogen concentration affected the coupling between methanogenesis and growth in at least two respects. (i) The microorganism could adopt two distinct theoretical maximal growth yields ($Y_{\text{CH}_4, \text{max}}$), notably approximately 3 and 7 g (dry weight) of methane formed mol⁻¹, for growth under low ($p_{\text{H}_2} < 12$ kPa)- and high-hydrogen conditions, respectively. The distinct values can be understood from a theoretical analysis of the process of methanogenesis presented in the supplemental material associated with this study. (ii) The in situ hydrogen concentration affected the “specific maintenance” requirements or, more likely, the degree of proton leakage and proton slippage processes. At low p_{H_2} values, the “specific maintenance” diminished and the specific growth yields approached $Y_{\text{CH}_4, \text{max}}$ indicating that growth and methanogenesis became fully coupled.

Most methanogenic archaea, including the *Methanothermobacter thermautotrophicus* used in the present study, derive their energy for autotrophic growth from the H₂-dependent reduction of CO₂ into methane. The pathways of methane formation, CO₂ fixation, and ATP synthesis are highly conserved among the different H₂-utilizing (hydrogenotrophic) methanogens (for reviews, see references 5, 6, 9, and 32 and additional information in the supplemental material). Nevertheless, different species display remarkable differences in specific growth yields (Y_{CH_4}), i.e., the amount of biomass formed per mole of methane produced at a given growth condition (Table 1). Y_{CH_4} values can be variable for a given species. Even maximal growth yields ($Y_{\text{CH}_4, \text{max}}$) seem to differ. $Y_{\text{CH}_4, \text{max}}$ represents the theoretical maximal growth yield that would be obtained if methanogenesis and growth are fully coupled.

Methanogens have to couple the processes of energy generation (methanogenesis) and biomass formation under highly diverse concentrations of their energy source, hydrogen. In environments such as anaerobic sediments and sewage digestors, hydrogen formed by obligate proton reducers is available at only very low levels (11, 37). In contrast, hydrogen concentrations can be high at sites where methanogens obtain the gas from H₂-producing fermentative microorganisms (29, 37). Un-

der laboratory conditions, the hydrogen availability of the cells depends on the gassing rates applied and the hydrogen-mass transfer capacity of the fermentative devices. In fed-batch systems, dissolved hydrogen partial pressures (p_{H_2}) continuously change over time as the result of increasing consumption rates by a growing biomass. Many authors observed that specific growth yields were relatively low when growth proceeded under hydrogen excess and that yields were highest under conditions of hydrogen limitation (7, 8, 12, 14, 18, 24, 27, 33, 34). Apparently, the degree of coupling between methanogenesis and growth depends on the in situ hydrogen concentration. In these studies, hydrogen-excess and hydrogen-limited conditions were imposed by changing the gassing rates or medium agitation. Unfortunately, with notable exceptions (12, 24), the hydrogen concentrations were not actually measured.

To investigate how methanogenesis and the growth of *M. thermautotrophicus* were coupled, we cultured the organism under a variety of hydrogen gassing regimens, while continuously recording the p_{H_2} value. We did so both in a fed-batch fermentor system, where conditions continuously change, and under the controlled conditions of a chemostat. In the fed-batch system the organism displayed a complex growth behavior comprising different growth phases that were each characterized by the distinct way that specific growth rates, growth yields, and methane-forming activities were interrelated. Both the fed-batch and the chemostat studies substantiated previous suggestions that specific growth yields depended on the dissolved hydrogen partial pressures and increased with decreasing p_{H_2} values. Quite remarkably, our work also suggests that *M. thermautotrophicus* may adopt two different maximal growth yields for growth under low- and high-hydrogen conditions.

* Corresponding author. Mailing address: Department of Microbiology, Faculty of Science, Radboud University of Nijmegen, Toernooiveld 1, NL-6525 ED Nijmegen, The Netherlands. Phone: 31-24-3653437. Fax: 31-24-3652830. E-mail: J.Keltjens@science.ru.nl.

† Supplemental material for this article may be found at <http://aem.asm.org/>.

∇ Published ahead of print on 1 December 2006.

TABLE 1. Specific (Y_{CH_4}) and maximal ($Y_{\text{CH}_4, \text{max}}$) growth yields of methanogenic archaea growing on hydrogen and CO_2

Organism	Amt (GDW mol of CH_4^{-1}) ^a		Source or reference
	Y_{CH_4}	$Y_{\text{CH}_4, \text{max}}$	
<i>Methanothermobacter marburgensis</i>	1.6–3.0		27
<i>Methanothermobacter thermautotrophicus</i>	0.6–1.6	3.1; 1.8 ^b	12, 24 This study
<i>Methanocaldococcus jannaschii</i>		3.6–3.7	33
<i>Methanothermococcus thermolithotrophicus</i>		3.33	7
<i>Methanobacterium bryantii</i> M.o.H.	2.48		21
<i>Methanobacterium formicicum</i>	3.5	6.0 ^c	2, 23
<i>Methanobrevibacter arboriphilicus</i>	2.68		36
<i>Methanosarcina barkeri</i>	6.37		35
<i>Methanosarcina</i> sp. strain 227	8.7		28

^a GDW, grams dry weight.

^b Calculated from data presented by the authors for growth under iron and hydrogen limitation, respectively.

^c Growth on formate.

MATERIALS AND METHODS

Chemicals. Gasses were supplied by Hoek-Loos (Schiedam, The Netherlands). To remove traces of oxygen, hydrogen-containing gasses were passed over a BASF RO-20 catalyst at room temperature; nitrogen-containing gasses were passed over a prerduced R3-11 catalyst at 150°C. The catalysts were a gift from BASF Aktiengesellschaft (Ludwigshafen, Germany). TCS (3,3',4',5-tetrachlorosalicylanilide) was purchased from Eastman Kodak (Rochester, NY). All other chemicals were of the highest grade available.

Fed-batch culturing. *M. thermautotrophicus*, formerly *Methanobacterium thermoautotrophicum* strain ΔH (DSM 1053), was grown in a 3-liter fermentor (MBR; B. Braun Biotech International GmbH, Melsungen, Germany) equipped with a gas-mixing device for the controlled gas supply, pH (Ingold; Elscolab BV, Maarsbroek, The Netherlands), hydrogen (see below), and temperature probes. The fermentor was filled with 1.5 to 2.5 liters of mineral medium (26), which was gassed with 80% H_2 –20% CO_2 (vol/vol). The medium contained the following constituents: NaHCO_3 (106 mM), KH_2PO_4 (50 mM), NH_4Cl (40 mM), MgCl_2 (0.2 mM), sodium resazurin (0.1 mg liter⁻¹), cysteine-HCl (4 mM), and $\text{Na}_2\text{S}_2\text{O}_3$ (4 mM), which served as reducing agents and sulfur sources. Trace elements were routinely added (0.1% [vol/vol]) from a concentrated standard solution based on the simple medium described by Schönheit et al. (26) containing the following (final medium concentration): nitrilotriacetate (150 μM), FeCl_2 (25 μM), NiCl_2 (5 μM), CoCl_2 (4 μM), and Na_2MoO_4 (1 μM). Occasionally (see below), the medium was supplied with a more complex trace elements mixture that, in addition to the standard compounds mentioned here, also contained (again, final concentrations are given) MnSO_4 (30 μM), CaCl_2 (9 μM), H_2SeO_3 (5 μM), H_3BO_3 (1.5 μM), CuSO_4 (0.4 μM), ZnSO_4 (0.35 μM), $\text{KAl}(\text{SO}_4)_2$ (0.2 μM), and Na_2WO_4 (0.1 μM). Culture took place at 65°C. Under the conditions applied, the medium pH was 7.0, except for the final linear growth stage, when the optical densities at 600 nm (OD_{600}) of the cells reached values of >3. Hereafter, the pH steadily decreased to become 6.7 at a high OD_{600} of 5 to 7.

After autoclaving, the medium was subsequently gassed (25 ml min⁻¹; 100 rpm) with 80% N_2 –20% CO_2 and 80% H_2 –20% CO_2 to determine the 0 and 80% settings and drifts of the hydrogen probe, respectively. Next, the fermentor was inoculated with 25 ml of a serum bottle culture in the medium described above that had been grown in a rotary shaking incubator operating at 200 rpm and at 65°C for 24 h. As soon as the methane formation had started in the fermentor, the stirring rate was set at 1,500 rpm and gassing with 80% H_2 –20% CO_2 was increased to the specified flow rate (v_{in} [ml min⁻¹]); the gassing rate was kept constant throughout the growth cycle. Analyses were started 5 to 12 h after adjustment of the gassing rate.

Chemostat culturing. Continuous culturing of *M. thermautotrophicus* used the equipment and mineral medium described above except that the 3.0-liter fermentor was operated as a chemostat with a culturing volume of 1.1 liter. Again, growth was performed at 65°C, and the cultures were gassed with 80% H_2 –20% CO_2 (vol/vol) at a stirring speed of 1,500 rpm. Dilution rates (D) were between 0.04 and 0.220 h⁻¹. Proper values were determined by measuring the volume of the outflow medium that had been collected during a known period of time.

TABLE 2. Steady-state cellular densities in chemostat cultures of *M. thermautotrophicus*^a

p_{H_2} (kPa)	Nutrient-controlled cultures				Hydrogen-controlled cultures			
	D (h ⁻¹)	v_{in}	pH	OD_{600}	D (h ⁻¹)	v_{in}	pH	OD_{600}
1	0.041	100	7.00	2.24	0.041	100	7.00	3.02
	0.085	120	7.10	2.19	0.087	100	6.92	2.45
	0.120	100	7.00	1.95	0.134	110	7.00	1.66
	0.171	100	7.00	1.02	0.171	115	7.00	1.15
5	0.048	150	6.95	2.64	0.041	250	6.90	4.35
	0.085	160	7.10	2.54	0.051	275	7.00	3.75
	0.123	175	6.90	2.78	0.123	275	6.90	2.78
	0.171	140	7.1	1.20				
15	0.085	250	6.95	2.20	0.041	350	6.98	6.50
	0.124	300	6.92	2.34	0.136	400	6.93	2.58
	0.164	300	6.95	1.63	0.164	400	6.95	2.30
	0.218	300	6.98	1.42	0.218	450	6.95	2.16
25	0.085	450	7.00	2.04				
	0.130	475	6.98	1.96	0.136	400	6.90	2.66
	0.155	450	6.96	2.00	0.164	400	6.95	2.32
	0.191	425	7.00	1.64				

^a The organism was grown as described in the text at the indicated hydrogen partial pressures (p_{H_2} , kPa), dilution rates (D , h⁻¹), 80% H_2 –20% CO_2 (vol/vol) gassing rates (v_{in} , ml min⁻¹), and pH values. Steady-state cellular densities were determined by measuring the $\text{OD}_{600} \pm 0.1$ at three different time points. The culturing resulted in one of two steady-state types, referred to as nutrient-controlled- and hydrogen-controlled-type cultures (see the text).

Gassing rates, which varied between 100 and 475 ml min⁻¹, were adjusted so that the dissolved hydrogen partial pressure under steady state was maintained at a desired value. A steady state is defined as the condition at which the OD_{600} of the culture, the dissolved hydrogen partial pressure, the rates of hydrogen consumption, and methane formation had become constant at a given gassing and dilution rate. The data presented were calculated from triplicate measurements that were performed three to four culture-volume changes after the establishment of a particular steady state. The growth conditions applied and the resulting steady-state OD_{600} values are summarized in Table 2. From the Table, it can be seen that the pH, which was not further controlled, was approximately constant for all conditions (7.0 ± 0.1).

Analytical procedures. Dissolved hydrogen partial pressures were monitored online with an amperometric p_{H_2} ($\text{Ag}_2\text{O}/\text{Ag}$) probe (24). The probe was prepared from a Clark-type oxygen electrode (Broadly Technologies Corp., Irvine, CA) and gave a linear response with respect to the dissolved hydrogen partial pressures in the 0 to 80% H_2 (0- to 80-kPa) range. Meter readings were corrected for a very small linear drift calculated from the slopes of the recorder during the gassing steps with 80% N_2 –20% CO_2 (0% H_2) and 80% H_2 –20% CO_2 prior to inoculation. The baseline signal (0% H_2) was checked at the end of the fed-batch growth cycle and at regular occasions during the course of the continuous culturing by stopping the gas supply. Previous studies showed that under the conditions applied the intracellular hydrogen concentration equals the hydrogen concentration in the medium (3, 4).

Outflow gas rates (v_{out} [ml min⁻¹]) were measured with a soap film flow meter. Hydrogen uptake rates (v_{H_2} [ml min⁻¹]) were calculated from the difference between the gas inflow and outflow rates ($v_{\text{in}} - v_{\text{out}}$). The relation follows from the stoichiometry of the process of methane formation from H_2 and CO_2 : $4 \text{H}_2 + \text{CO}_2 \rightarrow \text{CH}_4 + 2 \text{H}_2\text{O}$ (equation 1).

Methane production rates (v_{CH_4}) were determined by two methods. The first method simply used the difference between the in- and outflow gas rates at which $v_{\text{CH}_4} = (v_{\text{in}} - v_{\text{out}})/4$ (ml min⁻¹), which again follows from equation 1. It should be noted that the calculations ignore H_2 and CO_2 consumption for biomass formation. It is, however, known that less than 4 to 5% of the inflow gas is utilized for cell synthesis (24, 25). Alternatively, v_{CH_4} was determined by measuring the outflow gas rate and its methane content. Therefore, a 1-ml gas sample from the outflow gas was injected into a closed serum bottle containing 1 ml of the reference gas ethane; 0.1 ml-amounts of the gas mixture were analyzed on a HP 5890 gas chromatograph equipped with a Poropak Q column and a flame ionization detector (10). Methane production rates determined by gas chroma-

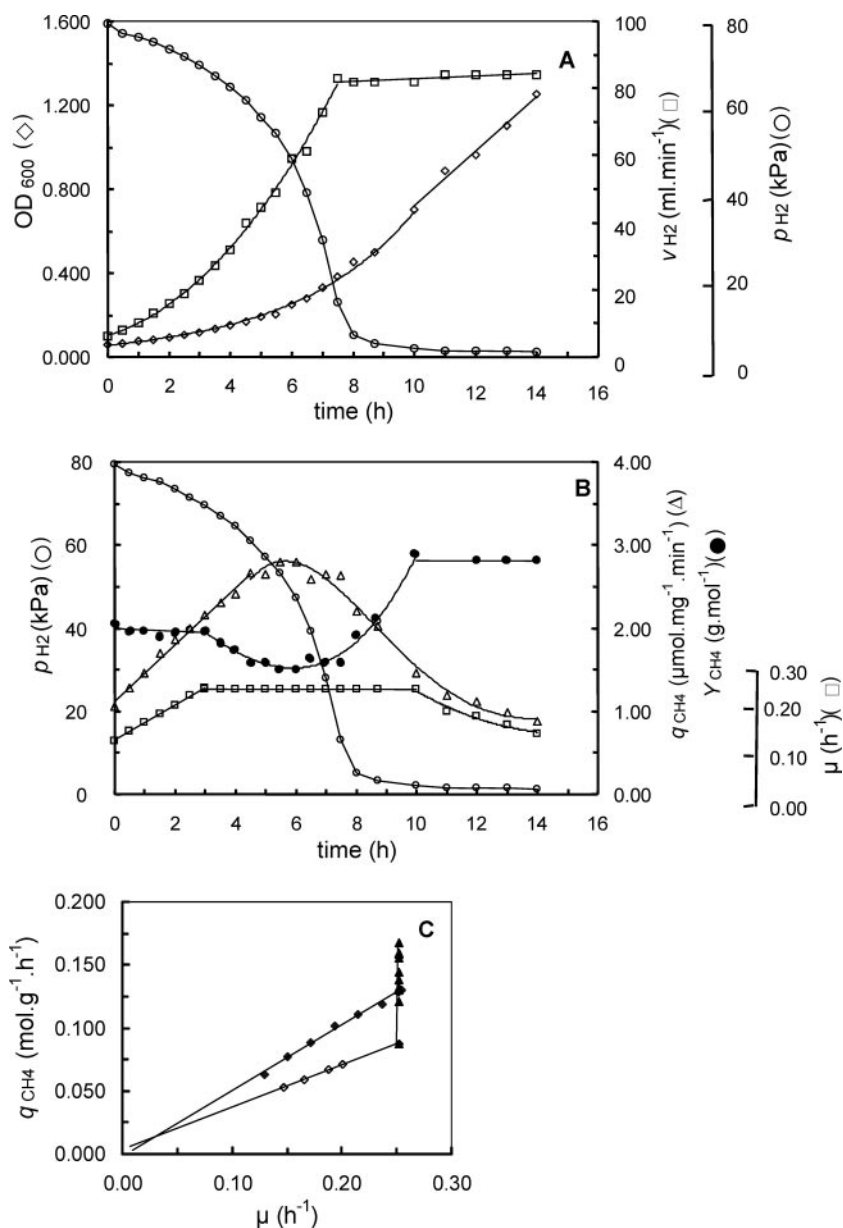


FIG. 1. Growth of *M. thermotrophicus* in a fed-batch reactor at a low gassing rate. The organism was cultured in 2.5 liters of mineral medium at a constant gassing rate of 107 ml min⁻¹ with 80% H₂-20% CO₂ (vol/vol). Measurements started ($t = 0$ h) 12 h after adjustment of the gassing rate. (A) Time course of cell growth measured as the OD₆₀₀, hydrogen uptake rate (v_{H_2}) and dissolved hydrogen partial pressure (p_{H_2}). (B) Time-dependent changes of the specific rate of methane formation (q_{CH_4}), specific growth rate (μ), specific growth yield (Y_{CH_4}), and p_{H_2} . (C) Relationship between q_{CH_4} and μ during the lag (\blacklozenge), exponential (\blacktriangle), and linear (\diamond) growth stages.

tography and by gas flow measurements alone deviated less than ca. 5% from each other.

At regular times, cells were anaerobically sampled from the fermentor for the OD₆₀₀ determination. Cell dry weights (DW) were calculated from the OD₆₀₀ values. Introductory experiments established the linear relationship between OD₆₀₀ and the DW content at which 1 liter of culture showing an OD₆₀₀ of 1 equaled 0.425 g DW of cells.

Determination of specific methane-forming activities, specific growth rates, and specific growth yields. Specific rates of methane formation (q_{CH_4} [mol of CH₄ g⁻¹ h⁻¹]) were calculated from the rates of methane formation and the corresponding biomass contents of the fermentor, measured as described above. Determination of the successive lag, exponential, and linear growth phases in fed-batch fermentor cultures was done as described in the supplemental material. We also specify here how specific growth rates (μ , h⁻¹) and specific

growth yields (Y_{CH_4} in g DW mol of methane formed⁻¹) were derived from primary data. It may be recalled that in a chemostat at steady state, the specific growth rate equals the dilution rate.

RESULTS

Growth characteristics of *M. thermotrophicus* in a fed-batch fermentor. When *M. thermotrophicus* was cultured in a fed-batch fermentor at a low 80% H₂-20% CO₂ gassing rate (107 ml min⁻¹) the cells grew, after a lag phase (see below), in an exponential way (3 to 10 h; Fig. 1A). As a result of increasing hydrogen consumption rates by the growing biomass, the

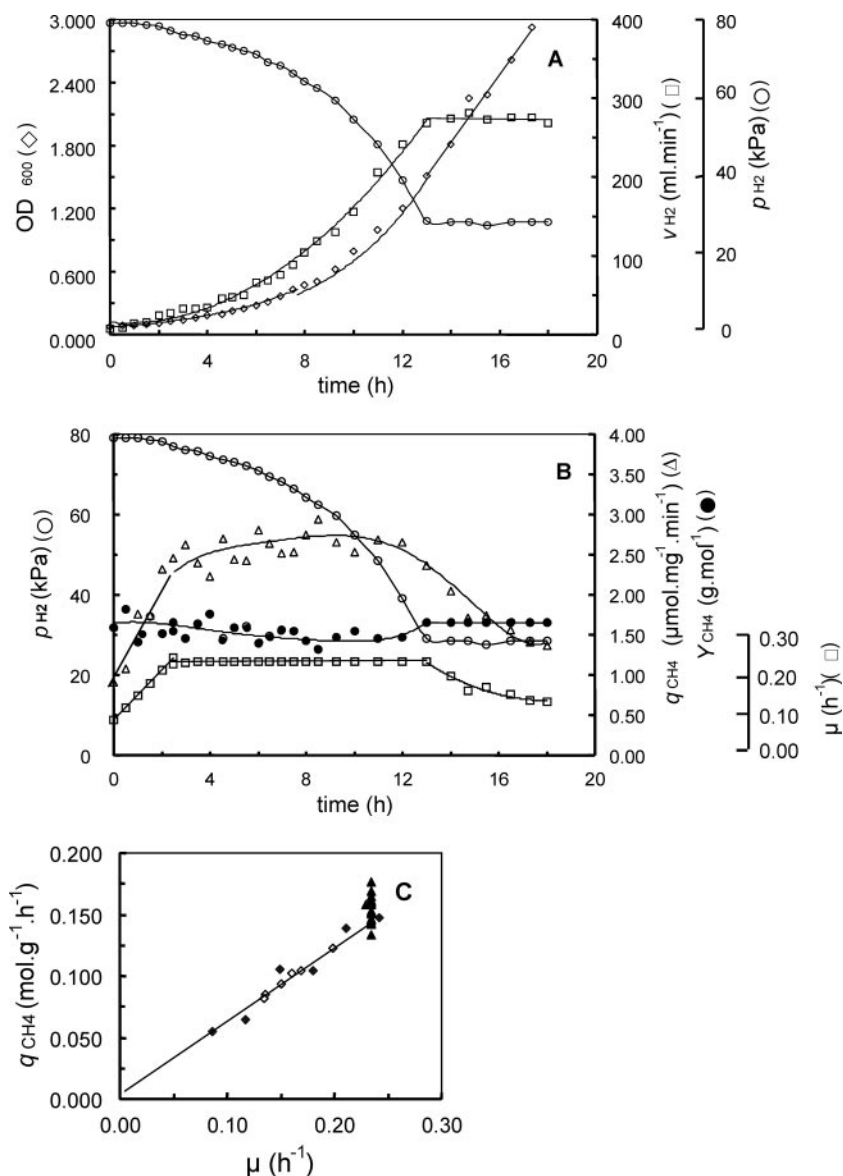


FIG. 2. Growth of *M. thermautotrophicus* in a fed-batch reactor at high gassing rate. The organism was cultured in 2.5 liters of mineral medium at a constant gassing rate of 428 ml min⁻¹ with 80% H₂-20% CO₂ (vol/vol). Measurements started ($t = 0$ h) 8 h after adjustment of the gassing rate. Panels A to C and symbols are as described in the legend to Fig. 1.

dissolved hydrogen partial pressure steadily decreased to become as low as 1 kPa. Before that time, the hydrogen consumption rate had become constant (84 ml min⁻¹), and 98% of the gas ended up in methane. When the p_{H_2} had reached the minimum at $t = 10$ h, the optical density increased linearly over time. This period is denoted as the linear phase. Apparently, growth now became limited by the H₂ supply. To test this, the organism was grown at a higher gassing rate (428 ml min⁻¹). The same growth behavior was found (Fig. 2A). Quite remarkably, p_{H_2} did not drop to low values during the linear growth stage, but it was maintained as high as 29 kPa. Again, the hydrogen consumption rate became constant ($v_{\text{H}_2} = 275$ ml min⁻¹), but the gas was only partly utilized. Further experiments showed that the p_{H_2} values could be manipulated by the H₂-CO₂ gassing regimen (Table 3). Depending on the hydro-

gen mass transfer characteristics, i.e., gassing rate/culture volume ratio and mixing intensity (number of impellers), steady p_{H_2} values were obtained during the linear growth phase that ranged between 1 and 59 kPa. Linear growth could proceed for prolonged periods of time (at least 72 h), at which OD₆₀₀ values of up to 7 to 10 were obtained (data not shown). Hydrogen consumption and methane production rates, as well as dissolved hydrogen partial pressures, however, remained constant throughout the whole period of linear growth.

Growth rates, growth yields, and methane-forming activities in the fed-batch fermentor system. As noted above, three consecutive growth phases could be discerned, notably the lag, exponential, and linear phases. The exponential phase is usually determined from the straight section of the graphs in which the (natural) logarithm of biomass (or OD) is plotted against

TABLE 3. Growth properties of *Methanothermobacter thermautotrophicus* in the fed-batch fermentor^a

Culture condition			Exponential phase				Linear phase	
v_{in} (ml min ⁻¹)	Vol (liter)	Mode	μ_{ex} (h ⁻¹)	$q_{CH_4,max}$ (mol g ⁻¹ h ⁻¹)	Δq_{CH_4} (mol g ⁻¹ h ⁻¹)	$Y_{CH_4,max}$ (g mol ⁻¹ CH ₄)	$p_{H_2,lin}$ (kPa)	$Y_{CH_4,lin}$ (g mol ⁻¹ CH ₄)
107	2.5	b	0.25	0.167	0.079	3.15	1	3.00
214	2.5	a	0.22	0.144	0.070	3.15	1	3.20
		b	0.24	0.127	0.034	7.05	4	2.20
		b	0.25	0.161	0.037	6.75	4	2.00
428	2.5	a	0.23	0.174	0.034	6.70	6	1.70
		b	0.23	0.177	0.035	6.70	29	1.65
	2.0	b	0.22	0.178	0.033	6.70	49	1.55
		1.5	b	0.22	0.188	0.033	6.70	59

^a *M. thermautotrophicus* was cultured at the indicated gassing rates and culture volumes. Abbreviations: v_{in} , gassing rate (80% H₂-20% CO₂ [vol/vol]); μ_{ex} , specific growth rate during exponential growth; $q_{CH_4,max}$, maximal specific methane-forming activity in the exponential phase; Δq_{CH_4} , difference between the maximal and minimal specific methane-forming activity in the exponential phase; $Y_{CH_4,max}$, theoretical maximal growth yield; $p_{H_2,lin}$, dissolved hydrogen partial pressure during linear growth; $Y_{CH_4,lin}$, specific growth yield during linear growth. Modes: a, one impeller mounted; b, two impellers mounted. $Y_{CH_4,max}$ and $Y_{CH_4,lin}$ were calculated as specified in the text and in the supplemental material (1).

time, the slope representing the specific growth rate during the exponential phase (μ_{ex}) (see also the supplemental material [1]). Deviation from linearity was always seen in the period preceding the exponential phase (lag period). Here, perfect straight lines were obtained, if the $\ln(OD_{600})$ values were plotted against the squared times (Fig. 3A, inset). As outlined in the supplemental material, this implies that the specific growth during the lag phase increases linearly in time (Fig. 1B and 2B). Also, the specific methane-forming activity increased linearly in time during this period (Fig. 1B and 2B). In fact, a plot of the q_{CH_4} values against the corresponding μ values showed a direct proportional relationship between both parameters, the slope representing the reciprocal of the specific growth yield (Y_{CH_4}), which now was constant (Fig. 1C, 2C, and 3A). The physiological meaning of these findings is that, after inoculation, cells adapt to the new growth condition by the uniform and concerted acceleration of their specific growth rate and specific methane-forming activity in a way that Y_{CH_4} remains fixed.

The specific growth rates became maximal at the entry of the exponential stage and remained constant throughout the particular stage (Fig. 1B, 2B, and 3A). The values did not significantly differ among the various gassing regimens (0.22 to 0.25 h⁻¹; doubling times of 2.8 to 3.1 h) (Table 3). However, the q_{CH_4} was not constant. Specific methane-forming activities initially increased to a maximum and declined thereafter. The decline occurred concomitant with the decrease in the dissolved hydrogen partial pressures, resulting from the increasing hydrogen uptake rates by the growing biomass (Fig. 1 and 2 and Table 3). Apparently, the physiology of the cells continuously changed, even at a constant growth rate.

After exponential growth, the cells entered the linear phase. During this stage, the specific growth rates and specific methane-forming activities, calculated by using the equations S.5 and S.6, respectively, in the supplemental material(1), decreased in parallel (Fig. 1B and 2B). Moreover, q_{CH_4} -versus- μ plots showed the direct proportional relationship as expected from equation S.8 (Fig. 1C, 2C, and 3B). The slope of the plots, which equals the reciprocal of the specific growth yield (equation S.8), varied with the dissolved hydrogen partial pressure

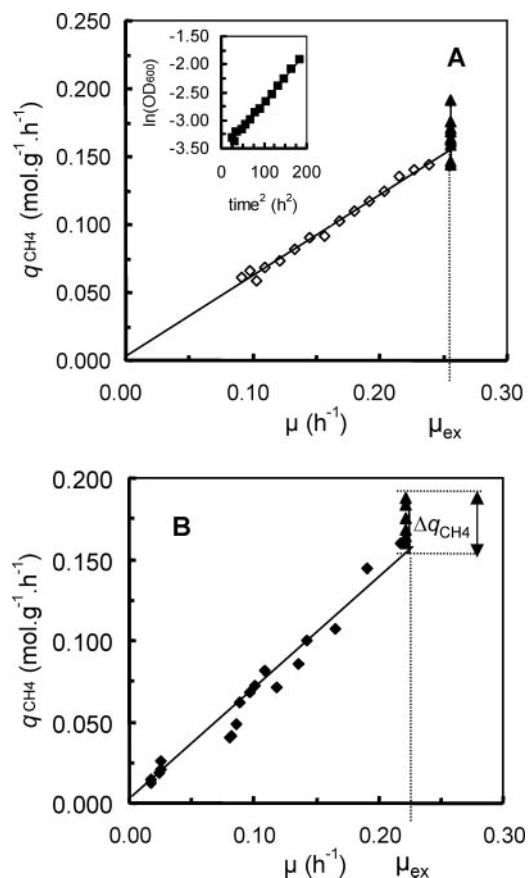


FIG. 3. Relationship between the specific rates of methanogenesis and specific growth rates during the lag (A), linear (B), and exponential growth phases. *M. thermautotrophicus* was cultured in 2.5 (A) and 1.5 (B) liters of mineral medium at a constant gassing rate of 428 ml min⁻¹ in 80% H₂-20% CO₂ (vol/vol). Measurements started 5 h (A) and 8 h (B) after adjustment of the gassing rates. In the inset of Fig. 3A, the $\ln(OD_{600})$ is plotted versus the squared time after inoculation. Lag (\diamond), exponential (\blacktriangle), and linear (\blacklozenge) growth stages are as indicated. μ_{ex} , specific growth rate during the exponential phase; Δq_{CH_4} , change between the maximal and minimal specific activities during the exponential phase.

during the linear phase. Y_{CH_4} values became higher at lower p_{H_2} values (Table 3). Thus, growth and methane formation became more tightly coupled at low hydrogen concentrations.

Maximal growth yields. As mentioned, q_{CH_4} took a maximal value in the course of the exponential stage and declined hereafter. The decline (Δq_{CH_4}) was relatively large, when the transition from the exponential to the linear phase took place below a p_{H_2} of 12 to 15 kPa (Fig. 1B, 1C, and 3B and Table 3). It then can be shown that $\Delta q_{\text{CH}_4} = \mu_{\text{ex}}/Y_{\text{CH}_4\text{max}}$, or $Y_{\text{CH}_4\text{max}} = \mu_{\text{ex}}/\Delta q_{\text{CH}_4}$, at which $Y_{\text{CH}_4\text{max}}$ and μ_{ex} represent the theoretical maximal growth yield at the start of linear growth and the exponential-phase-specific growth, respectively (see the supplemental material [1], equation S.9). The approach enables one to estimate $Y_{\text{CH}_4\text{max}}$ from a single fed-batch culture rather than from a series of continuous culture experiments (see below). The type of analysis suggested that *M. thermautotrophicus* may adopt two distinct $Y_{\text{CH}_4\text{max}}$ values, notably approximately 7 and 3 g DW mol of CH_4^{-1} formed during growth at high (>12 kPa) and low hydrogen partial pressures, respectively (Table 3). The same argumentation shows that the relationship $Y_{\text{CH}_4\text{max}} = \mu_{\text{ex}}/\Delta q_{\text{CH}_4}$ applies to the initial exponential phase as well. Here, Δq_{CH_4} represents the increase in the specific methane-forming activity at the onset of exponential growth versus $q_{\text{CH}_4\text{max}}$ (Fig. 1C, 2C, and 3A). Evaluation of the data demonstrated that the q_{CH_4} change, which occurs at a high p_{H_2} , also appeared to be related with a $Y_{\text{CH}_4\text{max}}$ of, again, approximately 7 g DW mol of methane $^{-1}$.

Transition from exponential to linear growth in the fed-batch fermentor. Linear growth and the shift from the exponential to the linear phase are intriguing phenomena. The obvious explanation would be energy or nutrient limitation, causing the progressive decrease in growth rate. The experiments under high hydrogen gassing conditions described above demonstrated that the shift to linear growth was not related to energy (hydrogen) limitation. Calculations indicate that CO_2 and bicarbonate were always present in large excess. Growth characteristics were not affected by an extra supply of medium constituents, including ammonia and reducing agents (thiosulfate and cysteine) (data not shown). We routinely used a simple trace element solution based on the medium described by Schönheit et al. (26). One may note that this trace solution apparently lacks metal ions, such as Zn^{2+} and Mn^{2+} , which may serve as cofactors for certain enzymes. To test whether or not the lack of a trace element was the limiting factor, a complex trace element solution containing all biological relevant metals in excess (see Materials and Methods) was added to a linear-phase culture growing on standard medium under high hydrogen gassing conditions (gassing rate, 428 ml min^{-1} ; p_{H_2} of 49 kPa at the time of addition). Indeed, the addition resulted in an initial 50% increase in the growth rate within 30 min. Growth, however, did not proceed to the point the hydrogen supply would have become limiting. Rather, cells kept on growing linearly, whereas the hydrogen consumption and methane production rates, as well as the p_{H_2} , were not significantly affected after the addition of the extra trace metals. Also, the growth characteristics of a complex trace elements culture, which had been pregrown on that medium for five transfers, were fully comparable to those of a culture on standard medium operated under the same high hydrogen gassing regimen. The characteristics particularly applied to the OD at

the entry of the linear phase, as well as to the v_{H_2} , v_{CH_4} , and p_{H_2} values during this phase. However, one difference was observed. The specific growth rate during the exponential phase of the complex trace elements culture was 50% higher. These observations indicate that nutrient limitation may limit the maximal growth rate. The limitation, however, does not offer an explanation for linear growth.

Interestingly, the shift could also be induced artificially by adding the uncoupler TCS (Fig. 4). Immediately after the addition of a small amount of TCS (2.8 nmol mg DW of cells $^{-1}$) to an exponentially growing culture ($\text{OD}_{600} = 1.0$), growth slowed down and the cell density increased linearly rather than exponentially in time (Fig. 4B). Simultaneously, the addition stimulated methane formation and hydrogen consumption, and, as a result of the latter, the decrease in p_{H_2} to approximately 1 kPa. For a comparison, the data shown in Fig. 2 of a culture operating under the same gassing regimen indicate that, starting from an OD_{600} of 1.0 and without TCS, exponential growth could have continued for an additional 3 h. In the particular culture (Fig. 2), p_{H_2} was maintained at 29 kPa

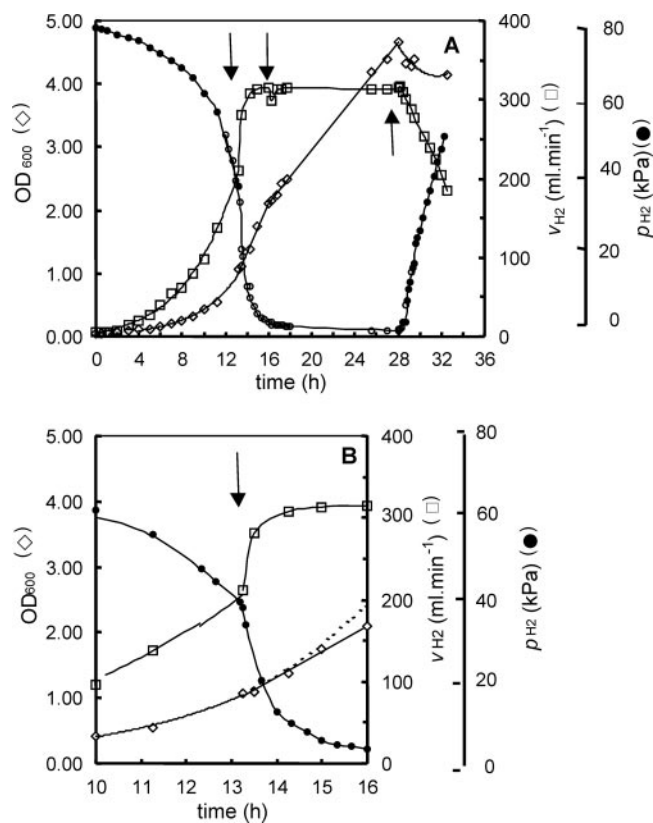


FIG. 4. Effect of TCS on growth of *M. thermautotrophicus*. The organism was cultured in 2.5 liters of mineral medium at a constant gassing rate of 428 ml min^{-1} with 80% H_2 -20% CO_2 (vol/vol), and the OD_{600} , hydrogen uptake rate (v_{H_2}), and dissolved hydrogen partial pressure (p_{H_2}) were monitored. Measurements started ($t = 0$) 8 h after adjustment of the gassing rate. At the times indicated by the arrows in panel A, 2.8, 11.4, and 120 nmol of TCS per mg DW of cells were added, respectively. In Fig. 4B, the period from 10 to 16 h is shown for better detail, at which TCS (2.8 nmol mg^{-1} DW) was added at $t = 13.5$ h (arrow). The dashed line represents the extrapolation of the trend curve for exponential growth ($t = 4$ to 13.5 h in panel A).

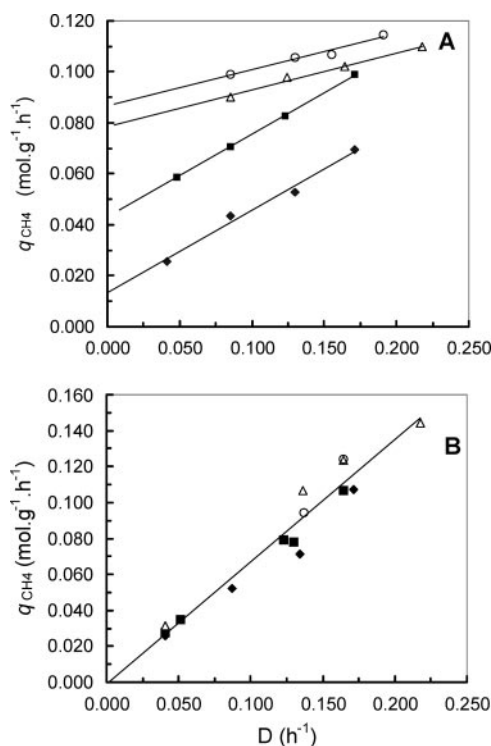


FIG. 5. Relationship between specific rate of methane formation (q_{CH_4}) and dilution rate (D) of “nutrient-controlled” (A) and “hydrogen-controlled” (B) chemostat cultures of *M. thermautotrophicus*. The organism was cultured as specified in Table 2 at the following dissolved hydrogen partial pressures (in kPa): 1 (\blacklozenge), 5 (\blacksquare), 15 (\triangle), and 25 (\circ).

during the linear phase. The stimulation of the respiratory (methanogenic) activity is a typical effect of uncouplers (1). A second pulse with TCS in a higher amount ($11.4 \text{ nmol mg DW of cells}^{-1}$) instantaneously provoked a further decline in growth. Again, cells kept on growing linearly, albeit at reduced growth rates. Since hydrogen was completely utilized at this time, methanogenesis was not further stimulated. The addition of excess TCS ($120 \text{ nmol mg DW of cells}^{-1}$) completely arrested growth. Methanogenesis and hydrogen utilization were also inhibited, and the progressive decline in hydrogen uptake was accompanied by a concomitant increase in the dissolved hydrogen partial pressure (Fig. 4). In the experiments, TCS was added as a methanolic solution, but the addition of methanol alone had no effect. These observations indicate that TCS acts both as an uncoupler of the energy metabolism (1) and as an uncoupler of methanogenesis and growth.

Coupling of methanogenesis and growth in continuous cultures of *M. thermautotrophicus*. To substantiate our findings from fed-batch experiments, we cultured *M. thermautotrophicus* in a chemostat at controlled dilution rates (D) and at defined dissolved hydrogen partial pressures. It was found that, after the change of the dilution rate and/or 80% H_2 –20% CO_2 gassing rate, the culture always got trapped in one of two types of steady state that could be distinguished on the basis of the steady-state ODs (Table 2) and the relationship between q_{CH_4} and the D (Fig. 5). In fact, the shift to a desired steady state could be experimentally controlled by the appropriate change in dilution and/or gassing rate, which might include a

predilution of the culture with fresh medium or by allowing cells density to increase by the intermediary stop of the medium supply.

Nutrient-controlled chemostat cultures. In the first type of culture (Fig. 5A), the OD_{600} values were approximately constant (~ 2) over the range of dilution rates and the p_{H_2} values tested (Table 2). The ODs, however, became lower at the higher dilution rates, where D approached the washout rate, i.e., the maximal specific growth rate in the particular medium (0.20 to 0.22 h^{-1}). This behavior is well known from classical chemostat culturing, where growth is determined by limitation of a nutrient in the liquid medium. As mentioned above, we routinely used a simple mineral medium, which could be limited in the presence of trace elements, such as Zn and Mn. The application in fed-batch fermentor cultures of a more complex trace element solution, containing all biological relevant metal ions in excess, resulted in an up to 50% increase in the specific growth rate (see above). This suggests that one or more of the extra trace metals now was growth limiting. Consequently, this type of culture is referred to as “nutrient controlled.” It should be noted that the steady-state OD_{600} values observed (~ 2) exceeded the ones accompanying the shift from the exponential into the linear phase in the fed-batch experiments ($\text{OD}_{600} = 0.7$ to 1.5) (Fig. 1A and 2A and data not shown). This substantiated our conclusion that the shift at the particular points was not due to a nutrient (trace element) limitation.

When the specific rates of methane formation of the “nutrient-controlled” cultures were plotted against D ($=\mu$) for the four different p_{H_2} values at which growth was monitored, four sets of straight lines were obtained (Fig. 5A). The data shown in the Fig. 5 are consistent with the coupling between q_{CH_4} and μ according to the linear Herbert-Pirt equation (2, 19, 22, 31; see the supplemental material for further information and for a theoretical derivation of the equation): $q_{\text{CH}_4} = (1/Y_{\text{CH}_4 \text{ max}})\mu + m$ (equation 2).

In the plots, slopes and the intercepts with the q_{CH_4} axis represent the reciprocal of $Y_{\text{CH}_4 \text{ max}}$ and the “specific maintenance term” (m), respectively. In fact, two distinct slopes could be observed depending on the p_{H_2} value. Linear regression analysis then yielded $Y_{\text{CH}_4 \text{ max}}$ values of 3.1 ± 0.3 and $3.1 \pm 0.1 \text{ g DW mol of CH}_4^{-1}$ for growth at a p_{H_2} of ca. 1 and 5 kPa, respectively. For growth at a p_{H_2} of 15 and 25 kPa, again, two equal $Y_{\text{CH}_4 \text{ max}}$ values were found, $6.9 \pm 0.5 \text{ g DW mol of CH}_4^{-1}$. The results are in excellent agreement with our findings from the fed-batch experiments, which suggested that $Y_{\text{CH}_4 \text{ max}}$ values of approximately 3 and 7 g DW mol of CH_4^{-1} for the growth of *M. thermautotrophicus* below and above p_{H_2} values of $\sim 12 \text{ kPa}$, respectively. It can also be seen from Fig. 5A that the “specific maintenance term” (m) increased with the hydrogen partial pressure at which growth had occurred. According to growth theory (7, 19, 31; see also the supplemental material), the specific growth yield (Y_{CH_4}), $Y_{\text{CH}_4 \text{ max}}$, μ , and m interrelate as follows: $1/Y_{\text{CH}_4} = (1/Y_{\text{CH}_4 \text{ max}}) + (m/\mu)$ (equation 3).

Thus, Y_{CH_4} diminishes with increasing m (at a given μ and $Y_{\text{CH}_4 \text{ max}}$). Otherwise stated, the specific growth yield decreased with increasing p_{H_2} , as was also concluded from the fed-batch experiments (Table 3).

Hydrogen-controlled chemostat cultures. In the second type of cultures (Fig. 5B), steady-state OD_{600} values were generally

higher compared to the “nutrient-limited” cultures operating at the corresponding dilution rates and hydrogen partial pressures (Table 2). At a given p_{H_2} , the OD_{600} decreased with increasing dilution rates. If compared for the same dilution rates, the values, however, increased with the H_2 - CO_2 gassing rate. This indicates that growth was now governed by the gas supply. Since CO_2 was also present in excess in the liquid medium as bicarbonate, the determining factor would be the H_2 supply. This type of culture is denoted here as hydrogen controlled. When steady-state q_{CH_4} values were plotted against the corresponding dilution rates, at which $\mu = D$, a direct proportional relationship between both parameters was observed (Fig. 5B) as follows: $q_{\text{CH}_4} = (1/Y_{\text{CH}_4})\mu$ (equation 4), where Y_{CH_4} should be constant. (Please note that the latter term refers to the specific growth yield rather than to a theoretical maximal growth yield.) A similar direct proportional relationship (equation 4) was found in our fed-batch experiments, notably during the lag and linear growth phases (Fig. 1C, 2C, and 3). Using linear regression analysis of the data presented in Fig. 5B and applying equation 4, an apparent and now p_{H_2} -independent Y_{CH_4} of 1.5 ± 0.1 g DW mol of CH_4^{-1} was calculated.

Interestingly, the culture of *M. thermautotrophicus* in the chemostat in the presence of the complex trace element mixture consistently resulted in only one type, the hydrogen-controlled type (data not shown). This held for all different dilutions (0.04 to 0.18 h $^{-1}$) and gassing rates (100 to 400 ml min $^{-1}$) applied. The q_{CH_4} -versus- D plot was the same as that shown in Fig. 3, except that the apparent Y_{CH_4} was somewhat higher (1.8 g DW mol of CH_4^{-1}). The findings support our conclusions that the growth of the cultures shown in Fig. 5A was determined by a limitation of a nutrient(s) in the liquid medium, viz. one or more trace elements, whereas Fig. 5B-type cultures were governed by the supply of the gaseous energy source, hydrogen. It should be noted, however, that, in the latter case, hydrogen was not the growth-limiting factor, except perhaps at low gassing rates (100 to 120 ml) and a concomitant low p_{H_2} of 1 kPa (Table 2), where 92 to 95% of the hydrogen was consumed. At the higher gassing rates and p_{H_2} values, H_2 was only partly utilized. Rather, it seemed that hydrogen controlled the particular mode of growth represented as the linear phase in the fed-batch system.

DISCUSSION

M. thermautotrophicus cultured in a fed-batch fermentor under different gassing regimens (gassing rates, gassing to culture volume ratios, mixing intensities) with 80% H_2 and 20% CO_2 displays a highly dynamic and complex growth behavior. However, it appeared that the organism always grew in a distinct order comprising the consecutive lag, exponential, and linear growth phases, which schematically can be represented by q_{CH_4} versus μ phase diagrams (Fig. 1C, 2C, and 3). In the chemostat, changes in hydrogen-gassing resulted in the establishment of one of two types of steady states. The central question in our study was how the supply of the energy source, hydrogen, determined the coupling between methanogenesis and growth. The effects were at least threefold. The hydrogen concentration affected (i) the specific (Y_{CH_4}) and theoretical

($Y_{\text{CH}_4 \text{ max}}$) maximal growth yields, (ii) the phenomenon of linear growth, and (iii) the so-called specific maintenance (m).

Specific growth yields increased when dissolved hydrogen partial pressures decreased. In the fed-batch system this was most apparent during the linear phase, when Y_{CH_4} and p_{H_2} became constant (Table 3). The continuous culture experiments shown in Fig. 5A fully supported this conclusion. Thus, methane formation and growth become more tightly coupled under conditions of reduced hydrogen availability. This finding is in agreement with observations by others (7, 8, 14, 17, 18, 27, 33), although the hydrogen concentrations had not been explicitly measured by those authors. A novel analytical approach applied to fed-batch growth suggested that $Y_{\text{CH}_4 \text{ max}}$ can take two distinct values, approximately 3 and 7 g mol $^{-1}$ of methane, respectively. Indeed, quite similar values of 3.1 ± 0.3 and 6.9 ± 0.5 g mol of methane $^{-1}$ were obtained by using the established continuous culture technique. The lower $Y_{\text{CH}_4 \text{ max}}$ applied when growth took place under conditions of low hydrogen. One may note that an $Y_{\text{CH}_4 \text{ max}}$ of 3.0 to 3.5 g DW mol of methane $^{-1}$ has been documented before for *M. thermautotrophicus* and other methanogens, notably during growth under H_2 -limited conditions (Table 1). In the fed-batch system, *M. thermautotrophicus* displayed specific growth yields at low hydrogen partial pressures (1 kPa) that were close to the theoretical maximum (Table 1), indicating that growth and methanogenesis became fully coupled. A $Y_{\text{CH}_4 \text{ max}}$ of ~ 7 g DW mol $^{-1}$ of methane, which was adopted when growth proceeded at $p_{\text{H}_2} > 12$ kPa, has as yet not been reported for *M. thermautotrophicus*. Importantly, the existence of the two distinct, hydrogen-dependent $Y_{\text{CH}_4 \text{ max}}$ values is predicted from a theoretical analysis of the process of methanogenesis presented in the supplemental material (2). The analysis suggests $Y_{\text{CH}_4 \text{ max}}$ values of 3.1 to 3.7 and 6.1 to 7.4 g DW mol of methane $^{-1}$ for growth below and above $p_{\text{H}_2} \sim 12$ kPa, respectively. The theoretical values favorably agree with the experimental values found here and by other authors. The change in $Y_{\text{CH}_4 \text{ max}}$ appears to be related to a change in proton-translocation stoichiometries associated with the H_2 -dependent reduction of the heterodisulfide of coenzyme M and coenzyme B (CoM-S-S-CoB), which takes place at a p_{H_2} of around 12 kPa (4; see also the supplemental material).

In the fed-batch system, growth proceeded after the exponential phase in a linear way for prolonged periods of time and p_{H_2} and as the hydrogen consumption and methane formation rates became fixed, depending on the hydrogen supplied (Table 3). As pointed out previously, linear growth could be the result of the limitation of a nutrient(s) in the standard medium used. However, growth experiments with media containing all biological relevant trace elements in excess seem to rule out this possibility. Quite remarkably, a shift toward linear growth was always also preceded by discrete decreases of the specific methane-forming activity at the end of the exponential phase in cultures supplemented with the complete trace set of elements (Table 1 and data not shown). The question is open as to whether the linear stage represents a growth phase by itself, namely, a growth mode, which is characterized, for instance, by the expression of specific genes. In this respect, the differential expression in *M. thermautotrophicus* of the *mrt* operon and the *hmd* gene coding for methylcoenzyme M reductase (MCR) isoenzyme II and H_2 -forming methylene- H_4 MPT dehydrogenase (HMD), respectively, and of the *mcr* operon and the *mdh*

gene are of interest. The latter two encode MCR I and coenzyme F₄₂₀-dependent methylene-H₄MPT dehydrogenase, respectively. Fed-batch experiments performed by Morgan et al. (14) demonstrated that *mrt* and *hmd* were expressed during exponential growth, whereas *mcr* and *mdh* transcripts were observed when the growth rate declined and the rate of methanogenesis became constant, which is typical for linear growth. It remains to be verified, however, if the differential expression of the above and other methane genes (13, 15, 16, 18, 20, 34) is connected to hydrogen deprivation, as has often been assumed, or to the shift in growth phases. Unfortunately, hydrogen partial pressures were not measured in the expression studies.

The culturing of *M. thermautotrophicus* in the chemostat resulted in two types of steady states that could be classified according to the steady-state optical densities (Table 2) and the q_{CH_4} - μ diagrams (Fig. 5). In fact, different research groups have studied the growth behavior of hydrogenotrophic methanogens using the chemostat technique and assuming methanogenesis and growth to be described by Pirt-like relations (equations 2 and 3). The results were, however, often not very clear and, on a number of occasions, contradictory. At least part of the confusion can be understood from the present findings. Continuous culture experiments performed with *Methanocaldococcus jannaschii* at varied hydrogen gassing rates demonstrated that the relations between q_{CH_4} and μ were most properly described by the Herbert-Pirt equation (equation 2), yielding an $Y_{\text{CH}_4 \text{ max}}$ of 3.6 to 3.7 g DW mol of CH₄⁻¹ (33). The simple linear relation did not hold for other studies done with *M. thermautotrophicus* and other methanogens (7, 8, 17). Inspection of the complex graphs presented by different authors shows them to actually consist of mixed curves, partly agreeing with the Pirt equations (equations 2 and 3). In other segments, specific growth yields had become constant, i.e., independent of specific growth rates, in agreement with equation 4. The data by von Stockar and coworkers (12, 24), who cultured *M. thermautotrophicus* (strain Hveragerdi) in the chemostat under H₂- and iron-limited conditions, are particularly interesting. A reevaluation of the graphs for iron and hydrogen limitation (12) reveals that the data can be most properly fitted by a simple Herbert-Pirt relationship (equation 2), such as in our "nutrient-controlled" cultures (Fig. 5A). From this, an $Y_{\text{CH}_4 \text{ max}}$ of 3.1 g DW mol of CH₄⁻¹ can be derived, which exactly equals our value at a low p_{H_2} . Moreover, the non-iron-limited culturing of the organism at defined hydrogen partial pressures resulted in the direct proportional and p_{H_2} -independent relationship between q_{CH_4} and μ , which is also seen in our Fig. 5B. Applying the Herbert-Pirt equation (equation 2), the Schill et al. (24) calculated a maximal growth yield of 0.019 mol of cells per mol of hydrogen consumed, equaling a $Y_{\text{CH}_4 \text{ max}}$ of 1.8 g DW mol of CH₄⁻¹, which, again, fully agrees with the value obtained here. Moreover, Liu et al. (12) concluded that the "specific maintenance" (m) would only be very small. However, as pointed out in the supplemental material (1), the slope of the q_{CH_4} versus the μ plot (cf. equation 4) represents the reciprocal of a now-constant specific growth yield (Y_{CH_4}) rather than of $Y_{\text{CH}_4 \text{ max}}$, whereas no conclusion can be drawn with respect to the size of m . The finding that cells grown in the chemostat under hydrogen-controlled (the present study) or under non-iron-limited conditions (12, 24) adopt a constant, apparently p_{H_2} -independent Y_{CH_4} needs further explanation.

According to the Pirt and Herbert-Pirt equations 2 and 3, methanogens couple the processes of methanogenesis and growth at variable hydrogen concentrations by adjusting $Y_{\text{CH}_4 \text{ max}}$ and the maintenance coefficient (m). $Y_{\text{CH}_4 \text{ max}}$ changes are discrete (see above). In order to establish the continuous changes in the relationships between specific growth rates, specific methane-forming activities, and specific growth yields that occur notably during fed-batch culturing (Fig. 1 to 3), m should be subjected to continuous changes as well, although in a nondiscrete fashion, thus permitting the elastic coupling between methane and biomass formation. In addition, maintenance coefficients had to be high at high hydrogen concentrations, resulting in a large degree of uncoupling of methanogenesis and growth. How cells control the "maintenance" changes is unclear. Unfortunately, the mechanistic meaning of the maintenance coefficient concept is not very clear either, being often simply defined as "any diversion of energy from growth to non-growth reactions" (22). A theoretical analysis of the process of methane formation suggests that the governing factor in "maintenance" is likely to be proton leakage or proton slippage (see the supplemental material [2]). The effect of the uncoupler TCS on the growth behavior (Fig. 4) supports this view. Furthermore, TCS seemed to induce the immediate shift from exponential to linear growth, indicating that the shift might be triggered by changes in the chemiosmotic status (internal pH, proton motive force) of the cells.

In conclusion, H₂ and CO₂ utilizing methanogens, such as *M. thermautotrophicus*, have to couple the process between methane formation and growth under highly variable concentrations of the energy source, hydrogen. Adaptation is associated with a change in $Y_{\text{CH}_4 \text{ max}}$, which apparently is related to the change in the proton translocation stoichiometry of the H₂-dependent reduction of CoM-S-S-CoB (4), giving rise to two theoretically predicted and experimentally verified $Y_{\text{CH}_4 \text{ max}}$ values of approximately 3 and 7 g DW mol of CH₄⁻¹ for growth under low ($p_{\text{H}_2} < 12$ kPa)- and high-hydrogen conditions, respectively. Furthermore, adaptation encompasses the adjustment of the "specific maintenance" requirements or, more likely, the degree of proton leakage and proton slippage processes. At low p_{H_2} , "specific maintenance" diminishes and specific growth yields (Y_{CH_4}) approach $Y_{\text{CH}_4 \text{ max}}$, indicating that growth and methanogenesis become fully coupled. In a fed-batch system, where dissolved hydrogen partial pressures change together with the changing uptake rates by growing biomass, *M. thermautotrophicus* displays a complex, yet defined growth behavior, comprising the consecutive lag, exponential, and linear growth phases, each of which is characterized by the ways specific growth rates, specific growth yields, and specific rates of methanogenesis are interrelated.

ACKNOWLEDGMENTS

The work of Linda de Poorter was supported by the Life Sciences Foundation (ALW), which is subsidized by The Netherlands Organization for Scientific Research (NWO).

We thank Henk de Haas from the Engineering Department for the development and testing of the hydrogen probe. We also greatly appreciate the assistance of Hasna el Habti in the growth experiments.

REFERENCES

1. Blaut, M., and G. Gottschalk. 1985. Evidence for a chemiosmotic mechanism of ATP synthesis in methanogenic bacteria. *Trends Biochem. Sci.* **10**:486-489.

2. Chua, H. B., and J. P. Robinson. 1983. Formate-limited growth of *Methanobacterium formicicum* in steady-state cultures. *Arch. Microbiol.* **135**:158–160.
3. De Poorter, L. M. I., W. J. Geerts, and J. T. Keltjens. 2005. Hydrogen concentrations in methane-forming cells probed by the ratios of reduced and oxidized coenzyme F₄₂₀. *Microbiology* **151**:1697–1705.
4. De Poorter, L. M. I., W. J. Geerts, A. P. R. Theuvenet, and J. T. Keltjens. 2003. Bioenergetics of the formyl-methanofuran dehydrogenase and heterodisulfide reductase reactions in *Methanothermobacter thermoautotrophicus*. *Eur. J. Biochem.* **270**:66–75.
5. Deppenmeier, U., T. Lienard, and G. Gottschalk. 1999. Novel reactions involved in energy conservation by methanogenic archaea. *FEBS Lett.* **457**:291–297.
6. Deppenmeier, U., V. Müller, and G. Gottschalk. 1996. Pathways of energy conservation in methanogenic archaea. *Arch. Microbiol.* **165**:149–163.
7. Fardeau, M.-L., and J.-P. Belaich. 1986. Energetics of the growth of *Methanococcus thermolithotrophicus*. *Arch. Microbiol.* **144**:381–385.
8. Fardeau, M.-L., J.-P. Peillex, and J.-P. Belaich. 1987. Energetics of the growth of *Methanobacterium thermoautotrophicum* and *Methanococcus thermolithotrophicus* on ammonium chloride and dinitrogen. *Arch. Microbiol.* **148**:128–131.
9. Ferry, J. G. 1999. Enzymology of one-carbon metabolism in methanogenic pathways. *FEMS Microbiol. Rev.* **23**:13–38.
10. Gijzen, H. J., C. A. M. Broers, M. Barugahare, and C. K. Stumm. 1991. Methanogenic bacteria as endosymbionts of the ciliate *Nyctotherus ovalis* in the cockroach hindgut. *Appl. Environ. Microbiol.* **57**:1630–1634.
11. Kramer, H., and R. Conrad. 1993. Measurements of dissolved H₂ in methanogenic environments with a gas diffusion probe. *FEMS Microbiol. Ecol.* **12**:149–158.
12. Liu, J.-S., N. Schill, W. M. van Gulik, D. Voisard, I. W. Marison, and U. von Stockar. 1999. The coupling between catabolism and anabolism of *Methanobacterium thermoautotrophicum* in H₂- and iron-limited continuous cultures. *Enzyme Microbiol. Technol.* **25**:784–794.
13. Luo, H.-W., H. Zhang, T. Suzuki, S. Hatori, and Y. Kamagata. 2002. Differential expression of methanogenesis genes of *Methanothermobacter thermoautotrophicus* (formerly *Methanobacterium thermoautotrophicum*) in pure culture and in cocultures with fatty-oxidizing syntrophs. *Appl. Environ. Microbiol.* **68**:1173–1179.
14. Morgan, R. M., T. D. Pihl, J. Nölling, and J. N. Reeve. 1997. Hydrogen regulation of growth, growth yields, and methane gene transcription in *Methanobacterium thermoautotrophicum* ΔH. *J. Bacteriol.* **179**:889–898.
15. Nölling, J., T. D. Pihl, and J. N. Reeve. 1995. Cloning, sequencing, and growth-phase-dependent transcription of the coenzyme F₄₂₀-dependent N⁵,N¹⁰-methylene tetrahydromethanopterin reductase-encoding genes from *Methanobacterium thermoautotrophicum* ΔH and *Methanopyrus kandleri*. *J. Bacteriol.* **177**:7238–7244.
16. Nölling, J., T. D. Pihl, A. Vriesema, and J. N. Reeve. 1995. Organization and growth phase-dependent transcription of methane genes in two regions of the *Methanobacterium thermoautotrophicum* genome. *J. Bacteriol.* **177**:2460–2468.
17. Peillex, J.-P., M.-L. Fardeau, R. Boussand, J.-M. Navarro, and J.-P. Belaich. 1988. Growth of *Methanococcus thermolithotrophicus* in batch and continuous culture on H₂ and CO₂: influence of agitation. *Appl. Microbiol. Biotechnol.* **29**:560–564.
18. Pennings, J. L. A., P. Vermeij, L. M. I. de Poorter, J. T. Keltjens, and G. D. Vogels. 2000. Adaptation of methane formation and enzyme contents during growth of *Methanobacterium thermoautotrophicum* (strain ΔH) in a fed-batch fermentor. *Antonie Leeuwenhoek* **77**:281–291.
19. Pirt, S. J. 1965. The maintenance energy of bacteria in growing cultures. *Proc. R. Soc. London Ser. B* **163**:224–231.
20. Reeve, J. N., J. Nölling, R. M. Morgan, and D. R. Smith. 1997. Methanogenesis: genes, genomes, and who's on first? *J. Bacteriol.* **179**:5975–5986.
21. Robertson, A. M., and R. S. Wolfe. 1970. Adenosine triphosphate pools in *Methanobacterium*. *J. Bacteriol.* **102**:43–51.
22. Russell, J. B., and G. M. Cook. 1995. Energetics of bacterial growth: balance of anabolic and catabolic reactions. *Microbiol. Rev.* **59**:48–62.
23. Schauer, N. L., and J. G. Ferry. 1980. Metabolism of formate in *Methanobacterium formicicum*. *J. Bacteriol.* **142**:800–807.
24. Schill, N., W. M. van Gulik, D. Voisard, and U. von Stockar. 1996. Continuous culture limited by a gaseous substrate: development of a simple, unstructured mathematical model and experimental verification with *Methanobacterium thermoautotrophicum*. *Biotechnol. Bioeng.* **51**:645–658.
25. Schill, N., and U. von Stockar. 1995. Thermodynamic analysis of *Methanobacterium thermoautotrophicum*. *Thermochim. Acta* **251**:71–77.
26. Schönheit, P., J. Moll, and R. K. Thauer. 1979. Nickel, cobalt and molybdenum requirement for growth of *Methanobacterium thermoautotrophicum*. *Arch. Microbiol.* **123**:105–107.
27. Schönheit, P. J., J. Moll, and R. K. Thauer. 1980. Growth parameters (K_s, μ_{max}, Y_s) of *Methanobacterium thermoautotrophicum*. *Arch. Microbiol.* **127**:59–65.
28. Smith, M. R., and R. A. Mah. 1978. Growth and methanogenesis by *Methanosarcina* strain 227 on acetate and methanol. *Appl. Environ. Microbiol.* **36**:870–879.
29. Smolenski, W. J., and J. A. Robinson. 1988. In situ rumen hydrogen concentrations in steers fed eight times daily, measured using a mercury reduction detector. *FEMS Microbiol. Ecol.* **53**:95–100.
30. Taylor, G. T., and S. J. Pirt. 1977. Nutrition and factors limiting the growth of a methanogenic bacterium (*Methanobacterium thermoautotrophicum*). *Arch. Microbiol.* **113**:17–22.
31. Tempest, D. W., and O. M. Neijssel. 1978. Eco-physiological aspects of microbial growth in aerobic nutrient-limited environments. *Adv. Microbiol. Ecol.* **2**:105–153.
32. Thauer, R. K. 1998. Biochemistry of methanogenesis: a tribute to Marjory Stephenson. *Microbiology* **144**:2377–2406.
33. Tsao, J.-H., S. M. Kaneshiro, S.-S. Yu, and D. S. Clark. 1994. Continuous culture of *Methanococcus jannaschii*, an extremely thermophilic methanogen. *Biotechnol. Bioeng.* **43**:258–261.
34. Vermeij, P., J. L. A. Pennings, S. M. Maassen, J. T. Keltjens, and G. D. Vogels. 1997. Cellular levels of factor 390 and methanogenic enzymes during growth of *Methanobacterium thermoautotrophicum* strain ΔH. *J. Bacteriol.* **179**:6640–6648.
35. Weimer, P. J., and J. G. Zeikus. 1978. One carbon metabolism in methanogenic bacteria. Cellular characterization and growth of *Methanosarcina barkeri*. *Arch. Microbiol.* **119**:49–57.
36. Zehnder, A. J. B., and K. Wuhrmann. 1977. Physiology of a *Methanobacterium* strain AZ. *Arch. Microbiol.* **111**:199–205.
37. Zinder, S. H. 1993. Physiological ecology of methanogens, p. 128–206. *In* J. M. Ferry (ed.), *Methanogenesis, ecology, physiology, biochemistry, and genetics*. Chapman and Hall, New York, NY.